Journal of Applied Polymer Science

# Effects of co-hard segments on the microstructure and properties thermoplastic poly(ether ester) elastomers

**Tonghui Hao,[1]* Cheng Zhang,[1]* Guo-Hua Hu,[2] Tao Jiang,[1] Qunchao Zhang[1]**

[1]Hubei Collaborative Innovation Center for Advanced Organic Chemical Materials, Hubei University, Wuhan 430062, China

[2]Laboratory of Reactions and Process Engineering, CNRS–University of Lorraine, 1 rue Grandville, BP 20451 54001, Nancy Cedex, France

*Tonghui Hao and Cheng Zhang equally contributed to this article.

Correspondence to: Q. Zhang (E-mail: zhangqc76@sina.com)

**ABSTRACT:** A thermoplastic poly(ether ester) elastomer (TPEE) is composed of polyester hard segments and polyether soft segments. Polyester and polyether segments are often homopolymer segments. This work aims at incorporating poly(butylene phthalate (PBP) as co-hard segments in the hard segments of poly(butylene terephthalate) (PBT)-b-poly(tetramethylene oxide) (PTMO) thermoplastic elastomer, and investigating structures and properties of the resulting materials, denoted as (PBT-co-PBP)-b-PTMO. (PBT-co-PBP)-b-PTMO was synthesized from dimethyl terephthalate (DMT), dimethyl phthalate (DMP), PTMO ($M_n$ = 1000 g/mol), and 1,4-butanediol (BDO). The crystallinity of (PBT-co-PBP)-b-PTMO first decreased and then increased with increasing PBP content from 5% to 10% due to a decrease in the average sequence length of the PBT hard segments. Its elongation at break was increased by 200–350%. When the mass fractions of PBT and PBP were 42% and 8%, respectively, the (PBT-co-PBP)-b-PTMO showed the best performance in terms of permanent deformation, strength, and hardness whose values were 30%, 25 MPa, and 37 D, respectively. All the synthesized copolymers had good thermal stability with a decomposition temperature of 400°C or so. © 2016 Wiley Periodicals, Inc. J. Appl. Polym. Sci. **2016**, *133*, 43337.

**KEYWORDS:** differential scanning calorimetry (DSC); elastomers; properties and characterization; thermal properties; thermoplastics

Received 23 August 2015; accepted 11 December 2015

**DOI: 10.1002/app.43337**

## INTRODUCTION

Incorporating polyether segments into polyesters is an effective method to improve properties of the latter.[1–3] An early example is thermoplastic poly(ether ester) elastomers (TPEE) which were commercialized for the first time in 1972. Unlike conventional elastomeric materials, TPEE exhibit good processability, good solvent resistance, good biodegradability, and good heat resistance owing to their unique micro-phase separated structures.[4,5] As such, they have found wide spread applications in electronics, automotive industries, and skin tissue engineering, etc.[6–9]

Various types of TPEE have been developed.[10,11] A typical one is a copoly(ether ester) composed of poly(butylene terephthalate) (PBT) hard segments and poly(tetramethylene oxide) (PTMO) soft segments, denoted as PBT-b-PTMO. Its hard and soft segments are phase-separated due to thermodynamic immiscibility between them.[12,13] Thermodynamic immiscibility dictates, to a great extent, the crystallization behavior, morphology, thermal, and mechanical properties of the PBT-b-PTMO.[14] Many attempts have been made to improve its properties. Zhou *et al.* attempted to add $TiO_2$ or ZnO particles to the PBT-b-PTMO to improve its thermal stability, storage modulus, and mechanical properties.[15,16] Lin *et al.* studied the effect of incorporating *N,N′*-bis(2-hydroxyethyl)-pyromellitimide on fiber-forming and mechanical properties.[17–20] Johnson described the influence of the soft segment content and chain length on the physical properties of TPEE.[21]

However, specific applications such as medical infusion bags require even lower permanent deformation and lower hardness, while other excellent properties are retained.

To this end, this work attempts to introduce a concept called "co-hard segments". Half of the PBT hard segments of the PBT-b-PTMO are substituted by poly(butylene phthalate (PBP). The resulting copolymers are denoted as (PBT-co-PBP)-b-PTMO. Compared with the traditional thermoplastic poly(ether ester) materials, the (PBT-co-PBP)-b-PTMO copolymers synthesized in this work show better performances in many aspects. The relationship between the molecular structure, micro-structure, and properties of the (PBT-co-PBP)-b-PTMO copolymers is discussed.

## EXPERIMENTAL

### Materials

The reactants dimethyl terephthalate (DMT), dimethyl phthalate (DMP), 1,4-butanediol (BDO), and the catalysts tetrabutyl titanate (TBT) and magnesium acetate ($MgAc_2$) were all of chemical grade and were supplied by Sinopharm Chemical Reagent Co., China. Poly(tetramethylene oxide) (PTMO) with an average molar mass of 1000 g/mol was purchased from BASF, Germany. The antioxidant Irganox 1010 (pentaerythritol tetrakis[3-(3,5-di-tert-butyl-4-hydroxyphenyl)propionate] was supplied by Ciba. All the chemical substances were used without further purification.

### Synthesis of TPEE

(PBT-co-PBP)-b-PTMO was prepared by transesterification and then polycondensation in a well-dried steel reactor (Weihai Xingyu Chemical Machinery Co., China) equipped with a stirrer, a condenser, and a gas inlet. According to the recipe, a mixture of DMT, DMP, BDO, and PTMO as well as the antioxidant (0.5% of the total monomer mass) was charged to the steel reactor under nitrogen. The steel reactor was slowly heated up by an oil bath at 2°C/min. When the temperature reached 180°C, the catalysts TBT (0.1% of the total monomer mass) and $MgAc_2$ (0.02% of the total monomer mass) were added in. The transesterification reaction proceeded under gentle agitation and gentle nitrogen purge. The nitrogen purge aimed at sweeping out methanol, a byproduct of the transesterification reaction. When the amount of methanol reached 80% of the maximum theoretical mass, the transesterification reaction was considered to be finished. The steel reactor was then heated up to 250°C for polycondensation and the pressure inside the reactor was reduced to 10–20 Pa. The time necessary for the polycondensation depended on the molar mass of the resulting copolymer, which could be estimated by the torque on a dial. Finally, the copolymer was extruded from the reactor under nitrogen, cooled down in a water bath, and then granulated.

### Sample Preparation

Prior to any sample preparation, the (PBT-co-PBP)-b-PTMO TPEE granules were dried under vacuum at 60°C for 8 h and were then stored in a dry desiccator. The copolymer samples for fourier transform infra read (FT-IR) analysis were made in the form of films of about 0.5 mm thick by a 25 MPa Laboratory Heat Platens Press at a temperature of approximately 10°C above the melting temperature of the TPEE, and a pressure of 10 MPa for 30 s. Those for the nuclear magnetic resonance (NMR) analysis were dissolved in deuterated chloroform ($CDCl_3$) under ultrason till the complete dissolution of the copolymers. The copolymer/solvent ratio was 5% by wt/v. Those for the gel permeation chromatography (GPC) measurement were dissolved in 1,2,4-trichlorobenzene at 150°C with shaking. The copolymer concentration was about 2.5 mg/mL. The solutions were filtered by glass fiber filter paper with a pore size of about 1 $\mu$m. For the tensile and hardness tests, copolymers were prepared using an injection molding machine of type UM-80III, China at a temperature of approximately 20°C above the melting temperature of the TPEE. The injection pressure was 70 MPa and the holding temperature was 30 MPa for 30 s.

### Characterization

The FT-IR (PE-Spectrum one) and NMR (Inova 600) were used to characterize the chemical structure of the copolymers. For the NMR analysis, $CDCl_3$ was used as a solvent and tetramethylsilane (TMS) as an internal reference. The chemical shifts were reported in part per million. The number average molar masses ($M_n$), the weight average molecular weight (Mw), and polydispersity index (PDI = Mw/Mn) were calculated from GPC curves obtained by PL-GPC220 (Agilent Technologies). It was equipped with a HP1100 solvent delivery pump, a PD2040 triple detector array, and PL1110 wide molecular weight columns. The GPC measurements were carried out at 150°C using 1,2,4-trichlorobenzene as the eluent at a flow rate of 1 mL/min. The calibration was based on polystyrene standards with five different $M_n$ (6870, 841.7, 52.8, 28.77, and 2.94 kg/mol, respectively).

The melt flow index (MFI) of the TPEE was measured by a $\mu$PXRZ-400C melt flow meter (Education Instrument Factory of Jilin University, China), according to ISO 1133-2011. The temperature was set at 220°C.

Stress–strain curves were performed by a CMT4104 testing machine (SUNS, China) at a constant crosshead speed of 50 mm/min, according to the standard ISO 37-2011. Measurements were carried out at 25°C on dumbbell specimens. The length, width, and thickness of their middle portion were 33, 6.2, and 2 mm, respectively. At least five specimens were tested and the average values of the stress at yield, strain at yield, and permanent deformation rate at 100% elongation of those specimens were taken. The hardness of the specimens was performed on a Shore D apparatus of type Chuan Lu, China, according to ISO 7619-2011.

A polarized optical microscope (POM) of type POM (BX51 UK) instrument was used to characterize the crystalline structure of the copolymers. The cooling rate was 60°C/min. A differential scanning calorimeter of type differential scanning calorimetry (DSC, TQ-100) was used to investigate the melting behavior and crystallinity of the copolymers. The heating rate was 10°C/min and the atmosphere was nitrogen. The thermal stability of the copolymers was tested on a thermogravimetric analyzer (TGA) of type TASDT-Q600 at a heating rate of 10°C/min from room temperature to 600°C under nitrogen flow.

## RESULTS AND DISCUSSION

A series of TPEE copolymers were synthesized according to the compositions shown in Table I. The ratios between the hard and soft segments were always kept at 50/50. The resulting TPEE are expected to be linear multi-block copolymers and their soft and hard segments are more or less randomly distributed, as shown in Figure 1. They are composed of four different segments: PBT (DMT-BDO), PBP (DMP-BDO), poly dimethyl terephthalate-poly(tetramethylene oxide) PPT (DMT-PTMO), and poly dimethyl phthalate-poly(tetramethylene oxide) PTP (DMP-PTMO). They result from the reactions between DMT and BDO, DMP and BDO, DMT and PTMO, and DMP and PTMO, respectively.

### Molecular Structure and Molar Masses of TPEE

The chemical structures of the (PBT-*co*-PBP)-b-PTMO copolymers were confirmed by FT-IR and $^1$H NMR spectroscopies.

**Table I.** Compositions for the Synthesis of TPEE and Molar Masses of the Resulting TPEE

| Sample | DMT/DMP/PTMO (by mass) | n | $M_n$ ($10^4$ g/mol) | PDI | MFI (g/10min) |
|---|---|---|---|---|---|
| 1 | 50/0/50 | 7.2 | 3.6 | 2.1 | 10.0 |
| 2 | 45/5/50 | 4.9 | 3.4 | 2.3 | 13.6 |
| 3 | 44/6/50 | 4.2 | 3.2 | 2.2 | 13.0 |
| 4 | 43/7/50 | 3.7 | 3.5 | 2.5 | 11.0 |
| 5 | 42/8/50 | 3.4 | 3.0 | 2.2 | 10.0 |
| 6 | 41/9/50 | 3.5 | 3.1 | 2.4 | 9.5 |
| 7 | 40/10/50 | 3.7 | 2.9 | 2.3 | 9.0 |

n: Average sequence length of hard segments; Mn: number average molar masses; PDI:polydispersity index; MFI: melt flow index.

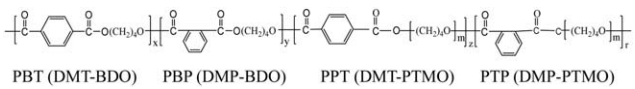


**Figure 1.** Chemical structure of (PBT-*co*-PBP-co)-b-PTMO random multi-block TPEE copolymers. It is composed of four different blocks of various lengths (z, y, z, and r).

Figure 2 shows a typical FT-IR spectrum of sample 5. The weak peaks at 2939 and 2854 $cm^{-1}$ are assigned to the asymmetric stretching and symmetric stretching of C–H of the soft segments. C=O stretching vibration and COO skeleton vibration appear at 1712 and 1266 $cm^{-1}$, respectively. The peak at 1098 $cm^{-1}$ is associated with the vibration absorption of ether bond (C–O–C) of the soft segments. The last peak at 724 $cm^{-1}$ is for the C–H vibration of the benzene ring.

Figure 3 shows a typical $^1$H NMR spectrum of sample 5, which corroborates the FT-IR spectra. Peak a at 8.09 ppm corresponds to the protons of terephthalate benzene ring, and those at 7.73 and 7.55 ppm (marked as h and g) are assigned to the two different protons of phthalate benzene ring. Peaks b (4.53 ppm) and d (1.97 ppm) correspond to the methylene protons of the hard segments, and peaks c (3.41 ppm) and e (1.62 ppm) correspond to the protons of the soft segments. The chemical shifts of the tetramethylene protons attached to the ester group of the soft segments are $b_1$ (4.35 ppm), $d_1$ (1.94 ppm), $e_1$ (1.73 ppm), and $c_1$ (3.46 ppm).

In $^{13}$C NMR (Figure 4) spectrum, peak a (165.75 ppm) corresponds to the carbon of the carbonyl group. Peaks b (134 ppm) and c (129.5 ppm) are for the non-protonated and protonated

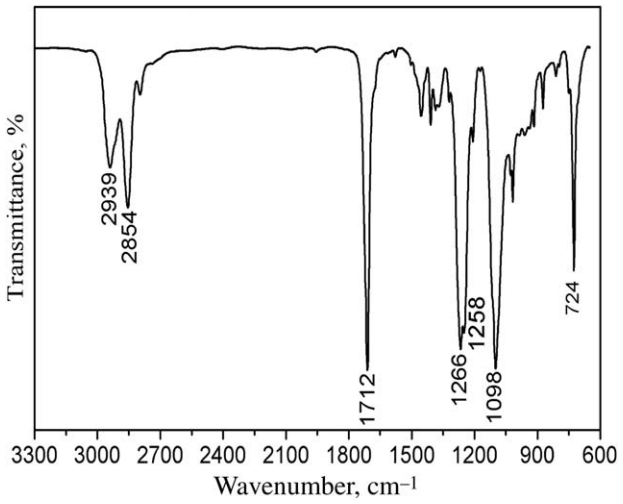


**Figure 2.** FT-IR spectrum of sample 5.

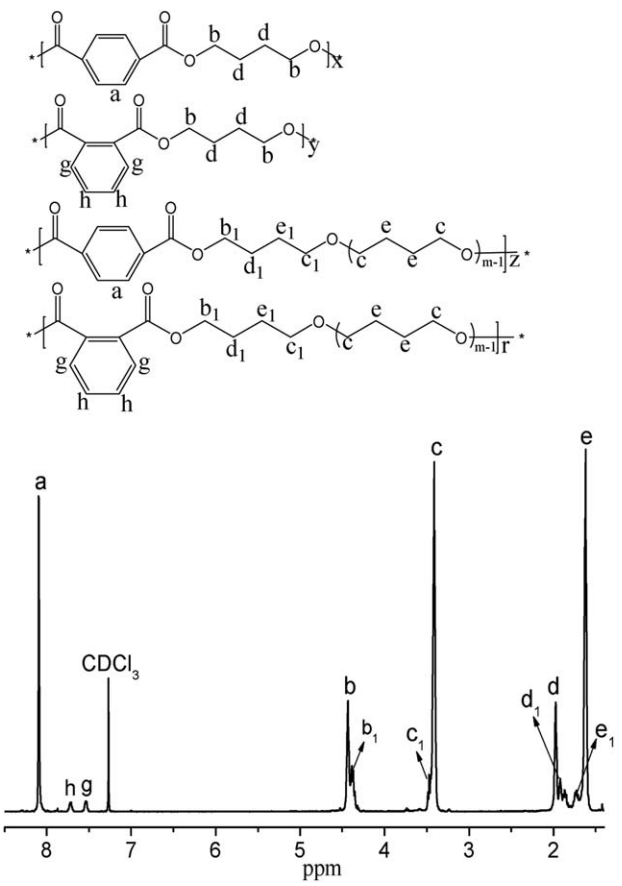


**Figure 3.** $^1$H NMR spectrum of sample 5 in $CDCl_3$.

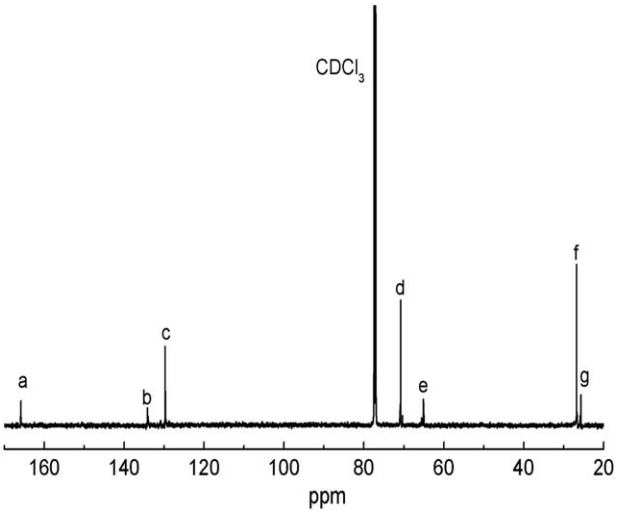


**Figure 4.** $^{13}$C NMR spectrum of sample 5 in $CDCl_3$.

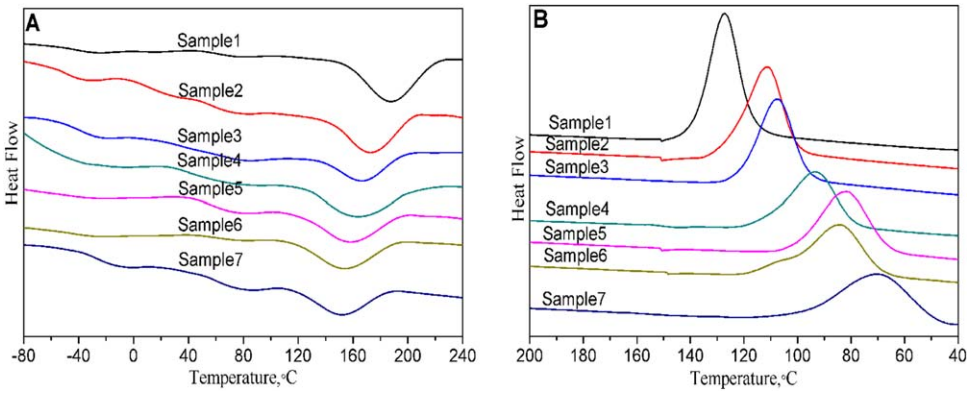


**Figure 5.** DSC curves of TPEE: (A) second heating cycle and (B) second cooling cycle. [Color figure can be viewed in the online issue, which is available at wileyonlinelibrary.com.]

carbons on the benzene ring, respectively. The chemical shifts at 70.6 ppm (peak d) and 25.4 ppm (peak f) are related to the methylene carbons of the soft segment. Those at 64.85 ppm (peak e) and 25.5 ppm (peak g) are due to the methylene carbons of the hard segment. The above results show that there are no side reactions occurring during the synthesis process.

Based on the peak areas of $^{1}H$ NMR spectra, the average sequence length of the hard segments, n, can be calculated by the following equation[22]:

$$\frac{n}{m-1}=\frac{I_b+I_d}{I_c+I_e}$$

where $I_b$, $I_c$, $I_d$, and $I_e$ are the integral areas of peaks b, c, d, and e; and m is the number of tetramethylene repeating units in the soft segments. Here m is 13.6 because the average molecular weight of the PTMO is 1000 g/mol. Similar calculations can be done by using the peak integral areas of $^{13}C$ NMR.

The above calculations show that n of the TPEE decreases from 7.2 to 3.4∼4.9 as the content of DMP (or PBP co-hard segments) increases from 0% to 10% by mass. As for their $M_n$ and PDI measured by the GPC, $M_n$ tends to decrease slightly with increasing content in DMP (or PBP co-hard segments) while PDI remains virtually constant (around 2.2). Except for the case where there is no DMP, the MFI gradually decreases from 13.6 to 9.0 when the DMP content increases from 5% to 10%. This is because MFI is directly related to the zero-shear rate viscosity of the TPEE, which depends both on its molar mass and its composition.

**Table II.** Thermal Properties of TPEE

| Sample | $T_{g1}$, °C | $T_{g2}$, °C | $T_m$, °C | $T_c$, °C | $\Delta H_m$, J/g | $\chi_c$, % |
|---|---|---|---|---|---|---|
| 1 | −33 | 62 | 191 | 127 | 28.9 | 20.0 |
| 2 | −34 | 65 | 179 | 111 | 24.0 | 16.6 |
| 3 | −32 | 67 | 174 | 106 | 22.8 | 15.8 |
| 4 | −33 | 69 | 170 | 99 | 21.8 | 15.1 |
| 5 | −34 | 70 | 165 | 81 | 20.7 | 14.3 |
| 6 | −32 | 72 | 156 | 84 | 21.2 | 14.7 |
| 7 | −32 | 74 | 156 | 69 | 21.7 | 15.0 |

$T_{g1}$, $T_{g2}$: glass transition temperatures of the soft and hard segments, respectively; $T_m$, $T_c$: melting and crystallization temperatures; $\Delta H_m$: enthalpy of crystallization; $\chi_c$: degree of crystallinity which is defined as the ratio of $\Delta H_m/\Delta H_m{}^0$, where $\Delta H m^0$ is the crystallization enthalpy of perfect crystalline component ($\Delta H_m{}^0$ = 144.5 J/g).

**Thermal Properties**

Figure 5 and Table II show the DSC traces of the TPEE during the second heating and cooling stages, respectively. The first cycle of heating and cooling was used to eliminate the thermal history of the samples. They reveal the existence of microphase separation in these multi-block copolymers due to the thermodynamic immiscibility between the hard and soft segments. From Figure 5(A), all TPEE exhibit three phases (two glass transition peaks and one melting peak). The glass transition peaks in the vicinity of −33°C ($T_{g1}$) and at 62∼74°C ($T_{g2}$) correspond to the amorphous PTMO phase and amorphous hard phase, respectively. The melting peak at 191∼155°C ($T_m$) results from the crystallized hard segments. The glass transition temperature ($T_{g1}$) is higher than that of the pure PTMO, which is −90°C, suggesting that the segmental mobility of the PTMO in the TPEE is more or less hindered by the presence of hard crystalline blocks. However, it does not change much with the variation of the content of the PBP co-hard segments. This implies

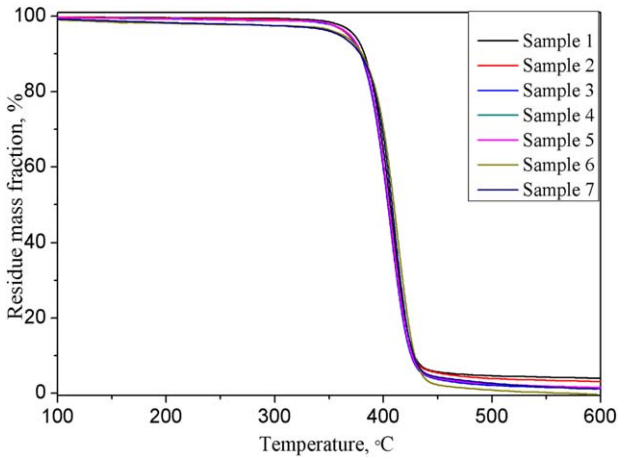


**Figure 6.** Thermal gravimetrical traces of TPEE under nitrogen for a heating rate of 10°C/min. [Color figure can be viewed in the online issue, which is available at wileyonlinelibrary.com.]

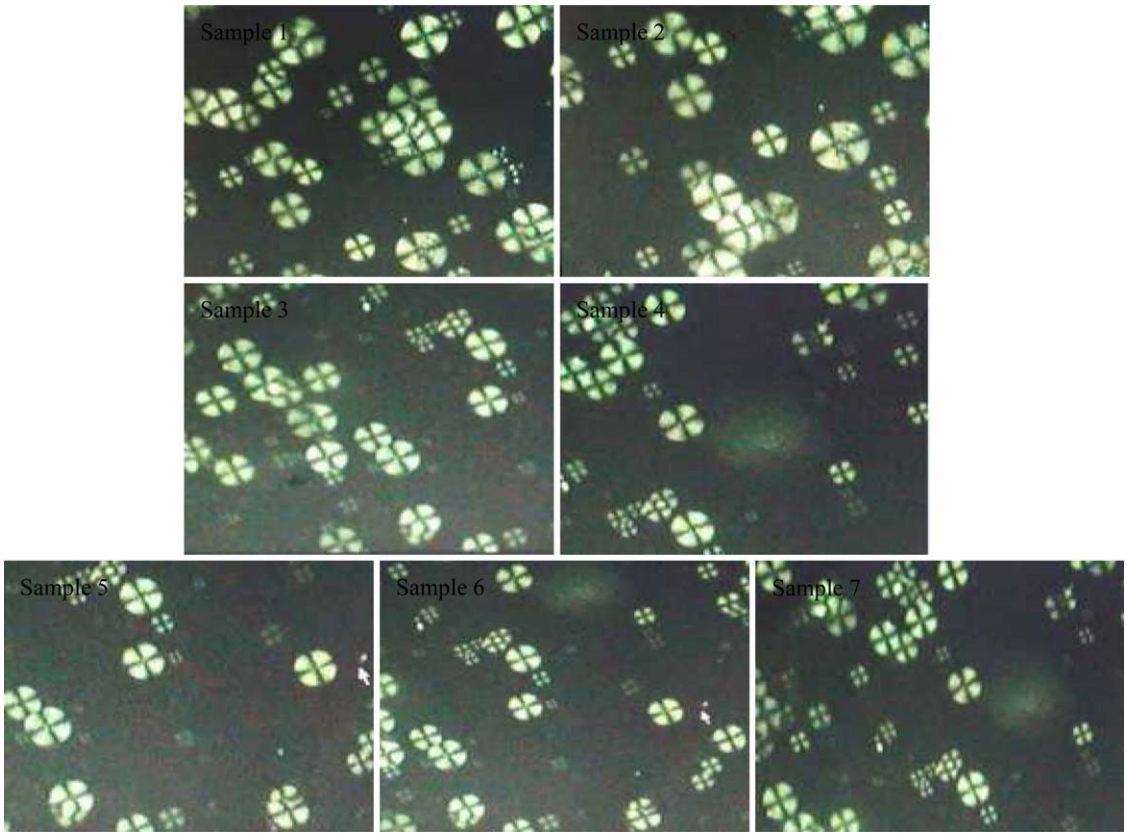


**Figure 7.** POM micrographs of TPEE. [Color figure can be viewed in the online issue, which is available at wileyonlinelibrary.com.]

that the PTMO forms a distinct phase.[23] The glass transition zones ($T_{g2}$) of some samples such as samples 3 and 6 are relatively wide, suggesting that the corresponding amorphous phases are mixtures of amorphous soft and hard segments. With increasing the PBP content, the melting temperature of crystallized hard segments decreased from 191 (sample 1) to 156°C (sample 7). This melting temperature depression can be ascribed to reduced crystalline lamellar thickness.

At the same time, the crystallinity decreases with increasing PBP content. The fact that both the melting temperature and crystallinity decrease with increasing PBP content can be attributed to less favorable crystallization conditions compared to the homopolymers.[12] As the PBP content increases, the average sequence length of hard segments first decreases. When it is 8% (sample 5), the average sequence length reaches a minimum of 3.4. A further increase in PBP content leads to an increase in the average sequence length. The change in crystallinity follows the trend of the average sequence length.

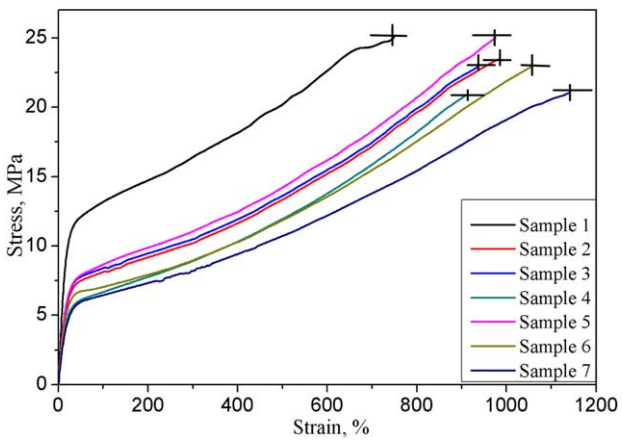


**Figure 8.** Stress–strain curves of TPEE. [Color figure can be viewed in the online issue, which is available at wileyonlinelibrary.com.]

The thermogravimetric experiments (Figure 6) show that the decomposition curves are basically the same for all samples, with small; differences in the initial decomposition temperature and the final residue content. The thermal stability of the samples is all good as they start to loss mass only when the temperature exceeds 350°C and accelerate the decomposition at about 400°C.

### Crystalline Morphology

Figure 7 shows POM micrographs of the TPEE. For all TPEE, on average spherulites are about 20 to 30 $\mu$m in diameter. Under the same crystallization conditions, they become smaller in size with increasing content in PBP co-hard segments. This is because an increase in the PBP content amounts to a decrease in the average sequence length of PBT hard segments, making the latter more difficult to crystallize.

### Mechanical Properties

Figure 8 shows the stress–strain curves of the TPEE. Each curve is the average of five specimens. They are typical of

**Table III.** Mechanical Properties of TPEE

| Sample | H (ShD) | $\varepsilon_b$ (%) | $\delta_b$ (MPa) | *E* (%) |
|---|---|---|---|---|
| 1 | 53 | 756 | 25.2 | 47.0 |
| 2 | 44 | 988 | 23.8 | 34.8 |
| 3 | 41 | 935 | 22.9 | 37.0 |
| 4 | 38 | 907 | 23.4 | 45.0 |
| 5 | 37 | 976 | 25.0 | 30.0 |
| 6 | 35 | 1056 | 23.0 | 35.0 |
| 7 | 34 | 1139 | 22.5 | 39.3 |

H: hardness; $\delta_b$: strength at break; $\varepsilon_b$: elongation at break; *E*: permanent deformation rate at 100% elongation.

thermoplastic poly(ether ester) elastomers: an elastic deformation with small elongations, followed by a decrease in the slope without an apparent yield point. The apparent yield point decreases when PBT is partly substituted by PBP, because of a decrease in crystallinity. Sample 1 shows a necking behavior after an elongation of 300% together with strain hardening till its fracture. Samples 5 and 6 deform uniformly till an elongation of 900%. The samples only exhibit a minor necking behavior at high elongation. The deformation below an elongation of 10% is reversible. When the elongation is from 50% to 300%, the deformation is no longer reversible because of the damage of crystalline structures. Some stress whitening phenomenon has appeared at high elongation after necking. This is attributed to strain-induced crystallization of soft segments, which becomes more important with increasing PTMO content or its length. The literature shows that it is an irreversible process.[24] As a matter of fact, the PTMO crystallites remain present even after the stress is released.[12]

Table III gathers the data of hardness, permanent deformation rate at 100% elongation, strength at break, and elongation at break for all seven TPEE. Substitution of part of PBT by PBP results in a decrease in hardness of TPEE from 53 D to 34 D and an increase in the elongation at break. These could mainly be attributed to a decrease in hard segment crystallinity. The permanent deformation rate at 100% elongation is reduced to a certain degree by the substitution of the PBT by PBP. However, the change in strength at break is not big, which is different from classical elastomers. The strength at break of the PBT-b-PTMO copolymer is 25.2 MPa. It remains in the range of 22.5 to 25 MPa when the PBP is incorporated in the copolymer. As for the elongation at break, it is high (more than 700%) for all the synthesized thermoplastic poly(ether ester) elastomers. The incorporation of the PBP further improves the elongation at break by 200–350%.

## CONCLUSIONS

This work has proposed a concept of co-hard segments for improving properties of thermoplastic poly(ether ester) elastomers of type poly(butylene terephthalate) (PBT)-b-poly(tetramethylene oxide) (PTMO). More specifically, half of the PBT hard segments is substituted by poly(butylene phthalate (PBP) and the resulting materials are denoted as (PBT-*co*-PBP)-b-PTMO. A series of (PBT-*co*-PBP)-b-PTM are synthesized by a conventional two-step process: transesterification followed by polycondensation. When the PBP content in (PBT-co-PBP)-b-PTMO is increased from 5% to 10%, its crystallinity first decreases and then increases due to the change in average sequence length hard segments. Its elongation at break could be increased by 200–350%. When the mass fraction of PBT and PBP were 42% and 8%, respectively, it shows the best performance in terms of permanent deformation, strength, and hardness

## ACKNOWLEDGMENTS

We are grateful for the financial support of the National High Technology Research and Development Program of China (No.2012AA06A111).

## REFERENCES

1. Huang, X.; Li, C. C.; Zheng, L. C.; Zhang, D.; Guan, G. H.; Xiao, Y. N. *Polym. Int.* **2009**, *58*, 893.
2. Colomines, G.; Robin, J. J.; Notingher, P.; Boutevin, B. *Eur. Polym. J.* **2009**, *45*, 2413.
3. Marija, V. V.; Vesna, V. A.; Biljana, P. D.; Milutin, N. G.; Jasna, D. *Polym. Int.* **2006**, *55*, 1304.
4. Cho, S.; Jang, Y.; Kim, D.; Lee, T. Y.; Lee, D. H.; Lee, Y. *Polym. Eng. Sci.* **2009**, *49*, 1456.
5. Lee, T. Y.; Lee, C. H.; Cho, S.; Lee, D. H.; Yoon, K. B. *Polym. Bul.* **2011**, *66*, 979.
6. Zhang, K.; Gao, L.; Chen, Y. *Polymer* **2010**, *51*, 2809.
7. Eberl, A.; Heumanna, S.; Kotekc, R. *J. Biotechnol.* **2008**, *135*, 45.
8. Gao, L.; Zhang, K.; Chen, Y. *Polymer* **2011**, *52*, 3681.
9. Vargantwar, P. H.; Brelander, S. M.; Krishnan, A. S.; Ghosh, T. K.; Spontak, R. J. *App. Phy. Let.* **2011**, *99*, 242901.
10. Szymczyka, A.; Nastalczyka, J.; Sablongb, R. J.; Roslaniec, Z. *Polym. Adv. Technol.* **2011**, *22*, 72.
11. Roslaniec, Z. In Handbook of Condensation Thermoplastic Elastomers; Fakirov, S., Ed., Wiley-VCH: Weinheim, **2005**; p 77.
12. Gabrielse, W.; Soliman, M.; Dijkstra, K. *Macromol.* **2001**, *34*, 1685.
13. Szymczyk, A. *Eur. Polym. J.* **2009**, *45*, 2653.
14. Bohwmick, A. K. Current Topics in Elastomers Research; CRC Press Taylor & Francis Group: Florida, **2008**; p 101.
15. Zhou, R. J.; Burkhart, T. *J. Mater. Sci.* **2011**, *46*, 2281.
16. Celebi, H.; Bayram, G.; Dogan, A. *J. Appl. Polym. Sci.* **2013**, *129*, 3417.
17. Lin, S. J.; He, W.; Lan, J. W.; Guo, R. H.; Shang, J. J.; Chen, S. *J. Macromol. Sci. Part A: Pure Appl. Chem.* **2013**, *50*, 416.
18. Shang, J. J.; Yao, G.; Lin, S. J.; Lan, J. W.; Huang, X.; He, W. *J. Macromol. Sci. Part A: Pure Appl. Chem.* **2013**, *50*, 1218.

19. Lin, S. J.; Shang, J. J.; Lan, J. W.; Guo, R. H.; Huang, X.; He, W. *J. Macromol. Sci. Part A: Pure Appl. Chem.* **2013**, *50*, 1060.
20. Lin, S. J.; Guo, R. H.; Lan, J. W.; Chen, S.; Shang, J. J. *J. Macromol. Sci. Part A: Pure Appl. Chem.* **2013**, *50*, 1052.
21. Johnson, V. J.; Byeong, K. M. *React. Funct. Polym.* **2013**, *73*, 1213.
22. Huang, W. C.; Wan, Y. B.; Chen, J. Y.; Xu, Q. Z.; Li, X. H.; Yang, X. M.; Li, Y. W.; Tu, Y. F. *Polym. Chem.* **2014**, *5*, 945.
23. Schmalz, H.; Guldener, V. V.; Gabrielse, W.; Lange, R.; Abetz, V. *Macromol.* **2002**, *35*, 5491.
24. Gabrielse, W.; Guldener, V. V.; Schmalz, H.; Abetz, V.; Lange, R. *Macromol.* **2002**, *35*, 6946.